



Preparation of a High Surface Area Nickel Electrode by Alloying and Dealloying in a ZnCl_2 -NaCl Melt

A. Katagiri^{*,z} and M. Nakata

Electrochemistry Laboratory, Faculty of Integrated Human Studies and Graduate School of Energy Science,
Kyoto University, Sakyo-ku, Kyoto 606-8501, Japan

An electrochemical method of preparing a high surface area nickel electrode by NiZn alloy formation and subsequent dealloying in ZnCl_2 -NaCl (60-40 mol %) at 450°C was studied. A nickel electrode was kept at 0.22 V vs. Zn in ZnCl_2 -NaCl(sat) where γ -NiZn alloy was formed, and then at 0.5 V where partial dealloying occurred to yield α -NiZn alloy. Scanning electron microscope observation showed that the microporous structure was formed on the surface. The roughness factor of a sample was determined to be 240 from the double layer capacitance obtained in the ac impedance measurement. Thickness, porosity, and pore size of the surface layer were estimated.

© 2003 The Electrochemical Society. [DOI: 10.1149/1.1595662] All rights reserved.

Manuscript submitted September 24, 2002; revised manuscript received March 10, 2003. This was in part Paper 1465 presented at the Philadelphia, Pennsylvania, Meeting of the Society, May 12-17, 2002. Available electronically July 17, 2003.

Zinc chloride-sodium chloride melts have relatively low liquids temperatures and exhibit characteristic properties due to the Lewis acidity of ZnCl_2 . We studied the electrochemical behavior of the nickel electrode in ZnCl_2 -NaCl (60-40 mol %) melt at 450°C by cyclic voltammetry (CV) and constant potential electrolysis, and reported that different types of NiZn alloys were formed depending upon the potential.¹ Equilibrium potentials of NiZn alloys of different structures and compositions were calculated from the thermodynamic data of zinc activity in alloys.² CV revealed that the anodic dissolution of zinc from NiZn alloys occurred on the potential scan in the positive direction. Formation of crevices and pores, and therefore the increase of surface area, were expected in the dealloying process. Preliminary experiments were performed in which γ -NiZn alloy was formed and then dealloyed to α -NiZn alloy, and the formation of a porous surface was verified by a scanning electron microscope (SEM).³ The present paper describes an electrochemical study of such alloying and dealloying, and presents some results of X-ray diffraction (XRD), X-ray fluorescence analysis, SEM observation, and electrochemical impedance measurements. Properties of the porous layer are also discussed.

High surface area nickel can be used as the cathode material for hydrogen evolution in water electrolysis and in chlor-alkali process.^{4,6} Several methods of preparing Raney nickel electrodes from NiAl and NiZn alloys have been proposed.⁷⁻¹⁴ For example, NiZn alloy coatings are made by electrodeposition in aqueous solutions⁷⁻¹⁰ and by reaction of nickel with zinc vapor (sherardizing).^{11,12} Zinc is then leached out in hot concentrated alkali hydroxide solutions to form high surface area nickel electrodes. The method proposed in this paper has an advantage; alloying and dealloying can be made by controlling the potential in the same electrolytic bath. Also the obtained product may have properties different from those made in aqueous solutions.

Experimental

Cathodic and anodic treatments of nickel were performed in a stationary ZnCl_2 -NaCl (60-40 mol %) melt at 450°C in a Pyrex glass cell. Nickel plates (Nilaco, 99.7%, 0.1 mm thick, 5 × 10 mm, total area 1 cm²) were used as the starting material. Prior to use they were electropolished in 1 M HCl at 0.5 A/cm² for 30 s. The counter electrode was a glassy carbon rod (Tokai Carbon, GC-20, 3 mm diam) separated from the main compartment by a glass frit. The reference electrode (RE) was molten zinc in ZnCl_2 -NaCl (saturated with NaCl) which was separated from the main compartment by a small piece of sodium β "-alumina. All potential values

were referred to this electrode. The equilibrium potential of zinc in ZnCl_2 -NaCl (60-40 mol %) at 450°C was 0.23 V vs. RE.

Zinc chloride was made as an aqueous solution from zinc carbonate and hydrochloric acid, and freed from heavy metal impurities. The solution was concentrated by heating, and the solidified material was vacuum dried at 200°C. The zinc chloride was further purified by sublimation at 450°C under vacuum. Sodium chloride was dried at 350°C under vacuum. ZnCl_2 -NaCl melt (60-40 mol %) was prepared from the thus obtained ZnCl_2 and NaCl.

Characterization of produced materials was performed by using a Shimadzu model XRD-6000 X-ray diffractometer with the Cu K α radiation, a Shimadzu model XRF-1500 X-ray fluorescence spectrometer. Microscopic observation was conducted with JEOL model JSM-T100, Hitachi S-3500H, and Hitachi X-900 SEMs. Electron probe microanalysis (EPMA) was carried out with a Shimadzu model EPMA-1600 instrument. AC impedance was measured with an NF Corporation model 5020 frequency response analyzer (FRA) and a Hokuto Denko HA-501 potentiostat.

Results and Discussion

Cathodic and anodic treatments of nickel electrodes.—In order to establish appropriate conditions for cathodic and anodic treatments, it is helpful to reinvestigate the voltammetric behavior of nickel. Figure 1 reproduces a cyclic voltammogram of a nickel wire electrode in ZnCl_2 -NaCl (60-40 mol %) melt at 450°C.¹ The Figure also shows the regions in which metallic zinc, γ -, β_1 -, and α -NiZn alloys are thermodynamically stable.^{1,2} A cathodic current observed at potentials below 0.28 V on the leftward scan is due to the formation of γ -NiZn alloy. An anodic current observed around 0.36 V on the rightward scan corresponds to the dissolution of zinc from γ -NiZn to yield β_1 -NiZn alloy. At potentials above 0.49 V an anodic reaction of β_1 -NiZn to form α -NiZn alloy occurs, and the dissolution of zinc from α -NiZn follows. Although the deposition of zinc can occur at potentials below the equilibrium potential of zinc ($E = 0.23$ V), the absence of the corresponding anodic current on the rightward scan indicates that metallic zinc, if any, reacts immediately with the nickel substrate to yield γ -NiZn alloy.

Based on the voltammetric results, cathodic treatment at $E_c = 0.22$ V and anodic treatment at $E_a = 0.50$ V were tried. The alloy phases expected were γ -NiZn at 0.22 V and α -NiZn at 0.50 V. Thus, a nickel plate (1 cm²), which had been electropolished in advance, was cathodically treated at 0.22 V until a quantity of electricity $Q_c = 35$ C/cm² passed. During this process (*ca.* 19 min), the color of the electrode was silver white. As shown in Fig. 2, the initial current of 70 mA/cm² dropped quickly to 40 mA/cm² after 2 min, and further decreased to 20 mA/cm² after 19 min. When the circuit was opened, the rest potential of the electrode was 0.27 V. Subsequent anodic treatment was conducted at 0.50 V until the cur-

* Electrochemical Society Active Member.

^z E-mail: katagiri.akira@a0016857.mbox.media.kyoto-u.ac.jp

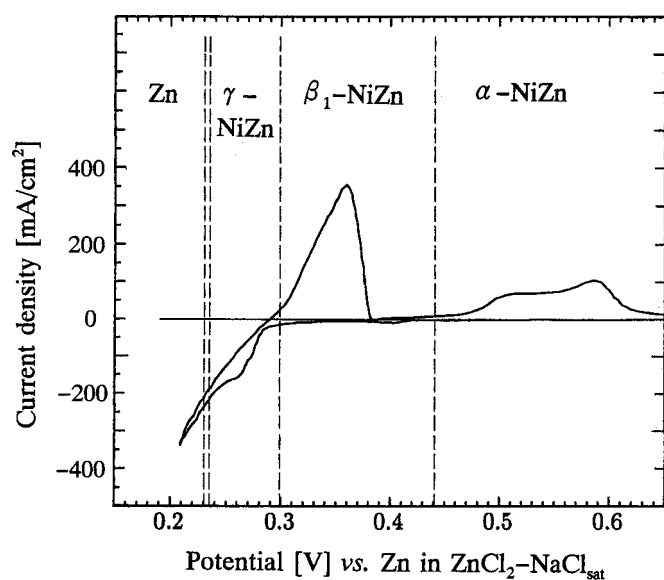


Figure 1. Cyclic voltammogram of a nickel wire electrode in a ZnCl_2 - NaCl (60-40 mol %) melt at 450°C . Scan rate, 0.2 V/s. The alloy phases and metallic zinc are thermodynamically stable in the regions divided by the broken lines.

rent dropped to zero. The surface of the electrode turned black immediately after the start of anodic treatment. As shown in Fig. 2, the anodic current changed in two steps. Thus the initial current of 200 mA/cm^2 decreased sharply, but a plateau of *ca.* 40 mA/cm^2 appeared after 2 min, which gradually decreased to zero. Such change in the anodic current suggests that two different processes occurred in dealloying. The quantity of electricity was $Q_a = (26 \pm 0.1) \text{C}/\text{cm}^2$.

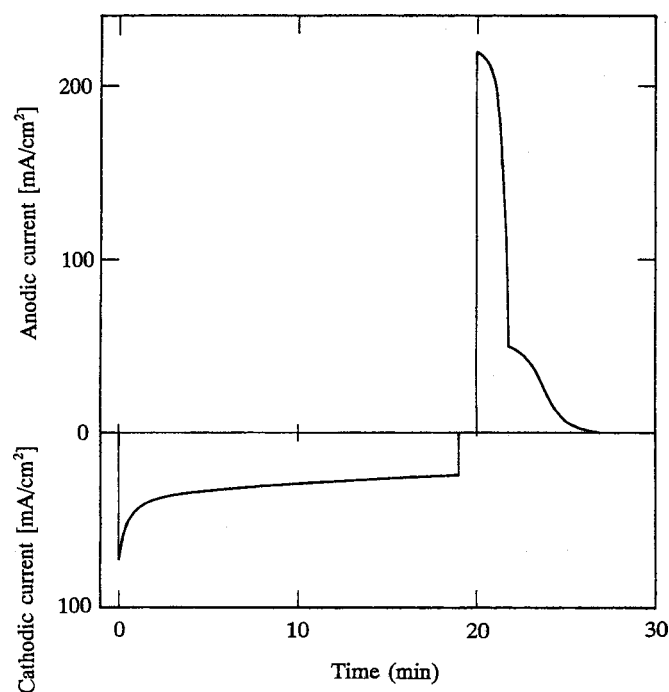


Figure 2. Variation of current during cathodic and anodic treatments of a Ni electrode in ZnCl_2 - NaCl (60-40 mol %) at 450°C . Cathodic treatment, $E_c = 0.22 \text{V}$, $Q_c = 35 \text{C}/\text{cm}^2$; anodic treatment, $E_a = 0.50 \text{V}$, $Q_a = 26 \text{C}/\text{cm}^2$.

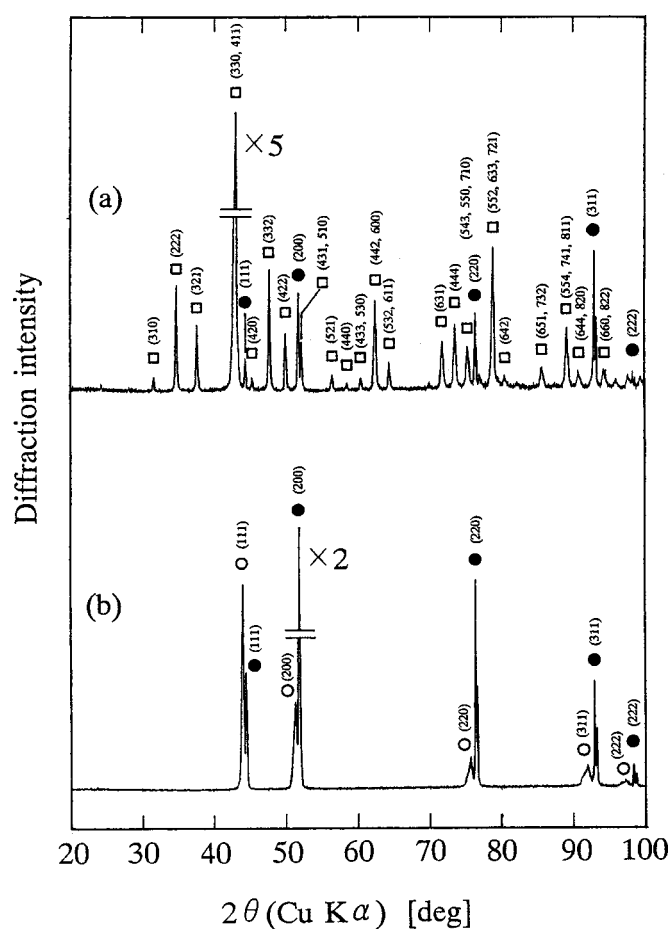


Figure 3. XRD patterns of (a) Sample I obtained by cathodic treatment ($E_c = 0.22 \text{V}$, $Q_c = 35 \text{C}/\text{cm}^2$) and (b) Sample II obtained by cathodic ($E_c = 0.22 \text{V}$, $Q_c = 35 \text{C}/\text{cm}^2$) and anodic ($E_a = 0.50 \text{V}$, $Q_a = 26 \text{C}/\text{cm}^2$) treatments in ZnCl_2 - NaCl (60-40 mol %) at 450°C . (●) Ni, (○) α -NiZn alloy, and (□) γ -NiZn alloy.

In order to investigate structural and property changes in cathodic and anodic treatments, two samples were prepared. Sample I was a nickel electrode treated only cathodically ($E_c = 0.22 \text{V}$, $Q_c = 35 \text{C}/\text{cm}^2$); sample II was another one treated cathodically ($E_c = 0.22 \text{V}$, $Q_c = 35 \text{C}/\text{cm}^2$) and then anodically ($E_a = 0.50 \text{V}$, $Q_a = 26 \text{C}/\text{cm}^2$). Both samples were rinsed with water and dried.

XRD.—XRD measurements were performed to investigate the crystallographic change in cathodic and anodic treatments. Figure 3a and b show the results of sample I and sample II, respectively. Sample I exhibits the diffraction patterns of γ -NiZn alloy and nickel, whereas sample II exhibits those of α -NiZn alloy and nickel. These results confirm that γ -NiZn alloy is formed by the cathodic treatment at 0.22 V, and anodic dissolution of zinc from γ -NiZn alloy occurs at 0.50 V leaving α -NiZn alloy. Table I summarizes the obtained lattice parameters which are in good agreement with the corresponding literature values.^{15,16}

In our previous work,¹ γ -NiZn alloy was formed on a nickel electrode in the constant potential electrolysis at 0.20 and 0.25 V, whereas the formation of α -NiZn alloy was not confirmed at 0.50 V. It seems that the formation of α -NiZn alloy occurs more easily in dealloying of γ -NiZn than in alloying of nickel at the same potential. As discussed previously,¹ the diffusion coefficient of zinc is larger in alloys of higher zinc concentration,¹⁷ and therefore zinc atoms diffuse out from the γ -NiZn alloy more easily than they diffuse into the nickel metal. Another point is the difference in the surface area. In the case of dealloying of γ -NiZn, crevices and pores

Table I. Lattice parameters of Ni, α -NiZn, and γ -NiZn alloys.

| Substance | Crystal structure | a_0 (present work) (Å) | a_0 (Ref. 15, 16) (Å) |
|----------------|-------------------|--------------------------------|-------------------------------|
| γ -NiZn | bcc ^a | 8.931 | 8.919 |
| α -NiZn | fcc ^b | 3.574 | 3.551 |
| Ni | fcc | 3.529 | 3.527 |

^a bcc is body-centered cubic.^b fcc is face-centered cubic.

develop due to the shrinking, and therefore the surface area increases, which accelerates the dealloying process. In the case of alloying of nickel, such mechanism does not work.

X-ray fluorescence (XRF) analysis.—Table II shows the results of XRF analysis of samples I and II. The intensity of the Zn K α signal was much larger in sample I than in sample II, whereas intensities of Ni K α and Ni K β signals were larger in sample II than in sample I. It is apparent that the zinc content of sample I was much larger than that of sample II, although quantitative interpretation is difficult for these layered materials because the observed X-ray intensity is the sum of signals from different depths. The results are consistent with the XRD data that sample I contains γ -NiZn alloy and sample II contains α -NiZn alloy.

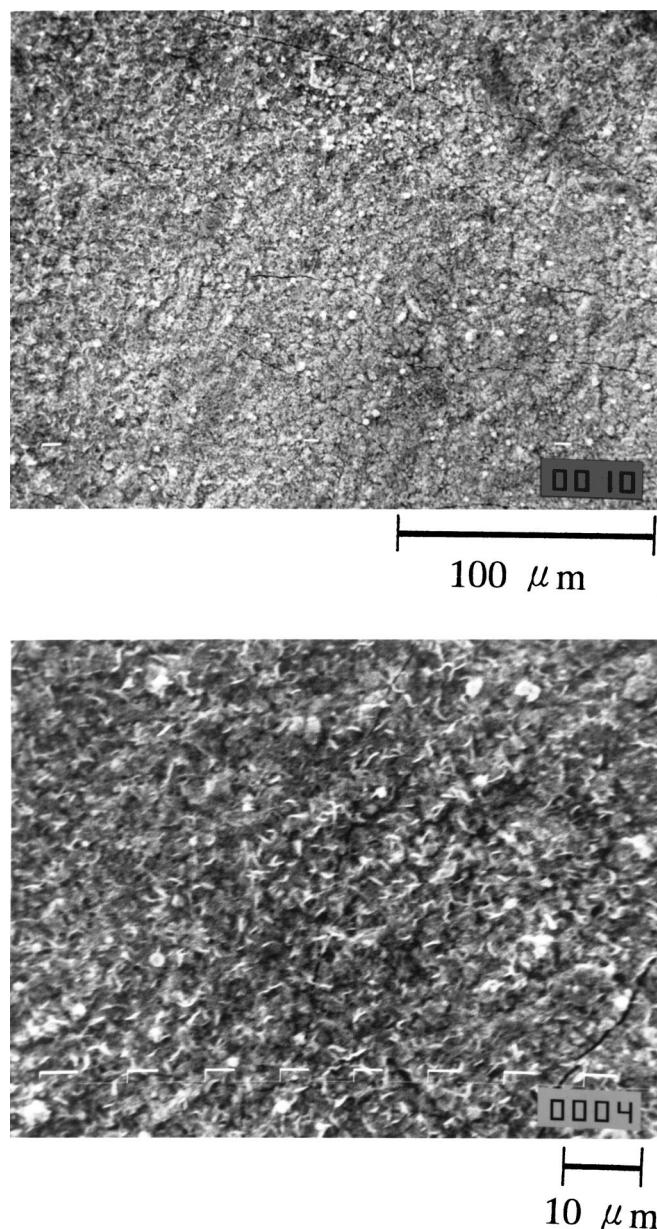
SEM observation and EPMA.—In order to reveal microscopic morphology of samples I and II, SEM observation was performed. Figures 4 and 5 show SEM photographs of the surfaces of sample I and sample II. While the surface of sample I seems compact with sparse microcracks, the surface of sample II has many crevices and pores, suggesting that the surface has a large internal area. Figure 6 shows SEM images of the surface of sample II in higher magnifications. The pore structure consists of interpenetrating phases of solid and void. Figure 7 shows the cross section of sample II. A porous layer of the thickness of about 10 μ m can be noticed on the top of the nickel substrate.

Distributions of nickel and zinc contents in the direction perpendicular to the electrode surface were measured by EPMA using cross-sectional samples. Figure 8 shows a backscattering electron image (BEI) of a cross section of sample I, together with the intensity profiles of Ni K α and Zn K α X-rays along a selected line indicated on BEI. X-ray signals provide information on local nickel and zinc contents with a resolution of 1 μ m. BEI of sample I exhibits a surface layer of 10–13 μ m in which intensity ratio of the Zn K α to Ni K α signal is about 2. Judging from XRD and XRF data, the surface layer is considered to be γ -NiZn alloy. It is noticed that another type of NiZn alloy (such as β_1 and α) does not exist in a thickness larger than the limit of resolution of EPMA.

Figure 9 shows EPMA results of a cross section of sample II. A porous layer is recognized in which the intensity ratio of the Zn K α to Ni K α signal is about 1/8. This porous layer apparently consists of α -NiZn alloy. Beneath this porous layer, there is no other alloy layer such as β_1 - and γ -NiZn. Comparing the surface layers of

Table II. Results of XRF analysis.^a

| Specimen | Fluorescent X-ray | Intensity (kcps) |
|-----------|-------------------|------------------|
| Sample I | Ni K α | 10.9 |
| | Ni K β | 2.0 |
| | Zn K α | 21.0 |
| Sample II | Ni K α | 30.5 |
| | Ni K β | 5.1 |
| | Zn K α | 2.1 |

^a Target = Rh; crystal = LiF.**Figure 4.** SEM photographs of the surface of sample I. See the captions of Fig. 3.

sample I and sample II, the intensity ratio of Zn K α to Ni K α signal has decreased by a factor of *ca.* 16. This change is due to the transformation of γ -NiZn to α -NiZn alloy.

Impedance measurements.—The roughness factor, which is the ratio of the true surface area to the geometric surface area, was determined from the double layer (dl) capacitance. Thus a piece of sample was soldered to a copper wire, and fabricated to the working electrode using a glass tube and Teflon seal tape. AC impedance of the electrode was measured in 1 M NaOH solution at 30 °C at the potential of -0.1 V vs. the reversible hydrogen electrode. The amplitude of AC signal was 10 mV, and the frequency was varied from 20 kHz to 100 mHz. The dl capacitance C_d was determined from the Cole-Cole plot of impedance data. Table III summarizes the obtained results. Assuming that the dl capacitance is proportional to the true surface area and taking the smooth nickel plate (not electropolished) as the reference, the roughness factor of sample II is calculated to be 240.

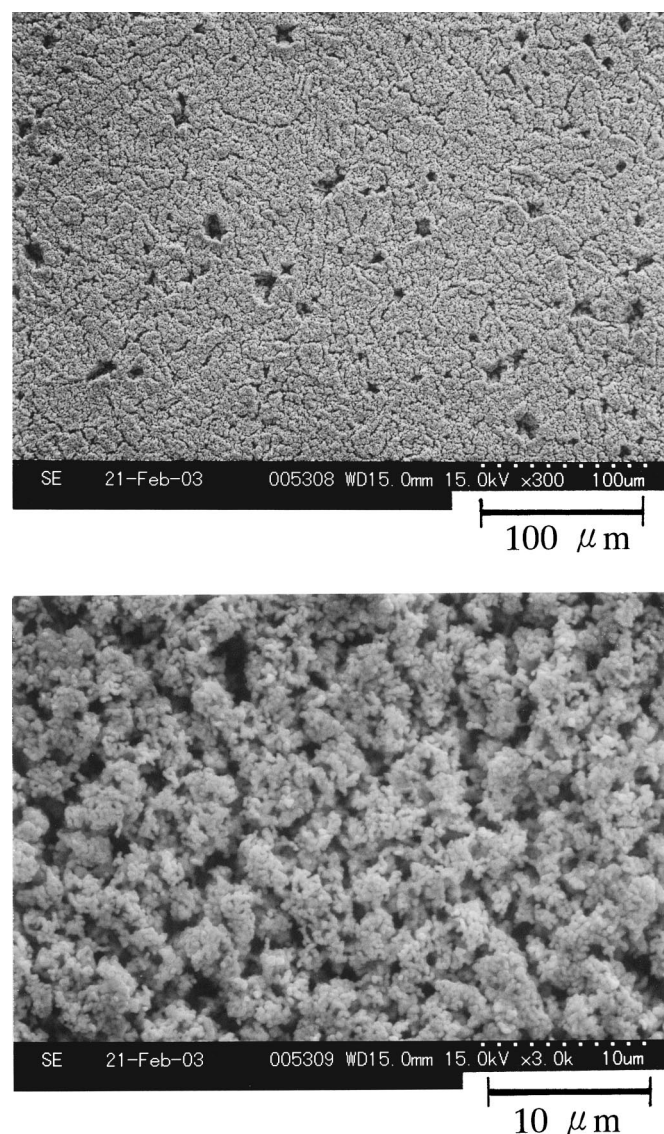


Figure 5. SEM photographs of the surface of sample II. See the captions of Fig. 3.

Discussion on the characteristics of porous layer.—The results obtained so far indicate that a single layer of γ -NiZn alloy is formed by the cathodic treatment at 0.22 V and subsequently a porous layer of α -NiZn alloy is formed by the anodic treatment at 0.50 V. Thus, the two-layer (α - and γ -NiZn) model proposed in a previous report¹⁸ is inadequate at least under stationary conditions. Now, processes of alloying and dealloying, and characteristics of the porous layer are discussed with the single layer model. Since the rest potential ($E = 0.27$ V) observed after the cathodic treatment is regarded as the equilibrium potential of the γ -NiZn alloy, its composition can be estimated from Nernst equation

$$E = E^0 - (RT/2F)\ln a_{\text{Zn}} \quad E^0 = 0.23 \text{ V} \quad [1]$$

Using the zinc activity data of the γ -NiZn alloy,² the mole fraction of zinc is obtained as $X_{\text{Zn}}(\gamma) = 0.81$; therefore the mole fraction of nickel is $X_{\text{Ni}}(\gamma) = 0.19$. Similarly, mole fractions of Zn and Ni in the α -NiZn alloy after the anodic treatment at 0.50 V are estimated to be $X_{\text{Zn}}(\alpha) = 0.12$ and $X_{\text{Ni}}(\alpha) = 0.88$. Table IV summarizes compositions of the γ - and α -NiZn alloys and related quantities.

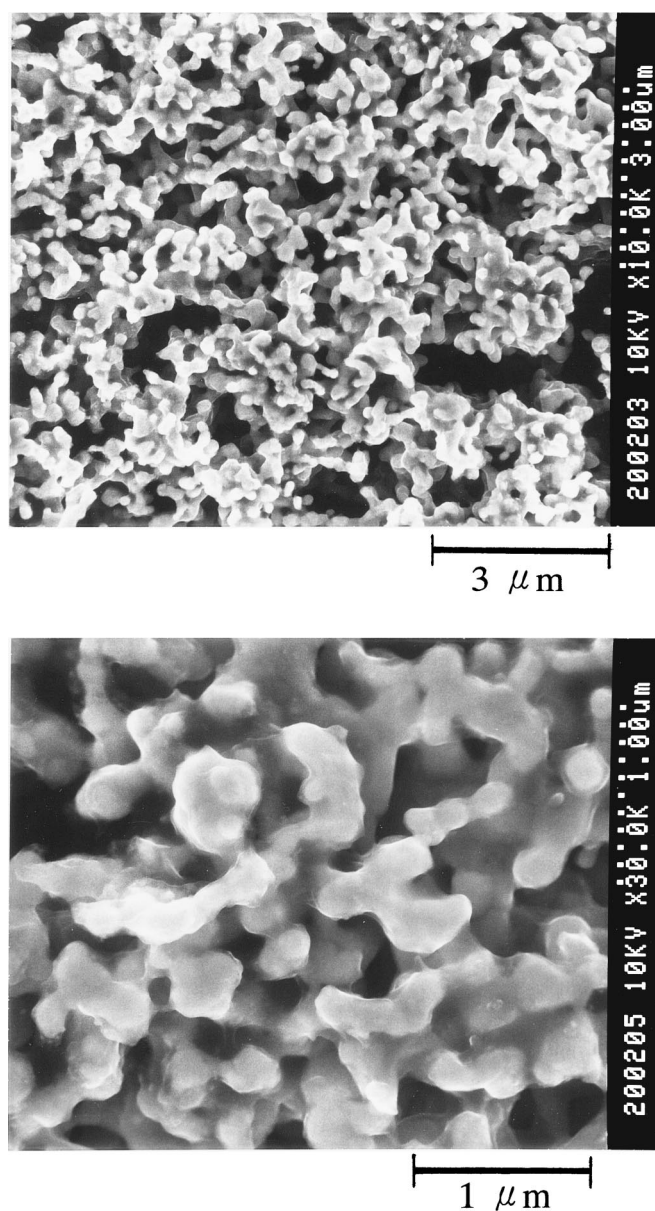


Figure 6. SEM photographs of the surface of sample II in high magnifications. See the captions of Fig. 3.

According to Faraday's law, the experimental data of $Q_c = 35 \text{ C/cm}^2$ gives the thickness of 18.5 μm of the γ -NiZn alloy. With this model, however, the percentage of dissolved zinc calculated from the compositions of γ - and α -NiZn alloys does not agree with that obtained from the quantities of electricity in cathodic and anodic treatments. Thus, on the one hand, the percentage of dissolved zinc, A , is expressed in terms of the mole ratios of zinc to nickel in γ - and α -alloys as

$$A = \frac{X_{\text{Zn}}(\gamma)/X_{\text{Ni}}(\gamma) - X_{\text{Zn}}(\alpha)/X_{\text{Ni}}(\alpha)}{X_{\text{Zn}}(\gamma)/X_{\text{Ni}}(\gamma)} \times 100 (\%) \quad [2]$$

Introducing the above-mentioned values yields $A = 96.8\%$. On the other hand, the percentage of dissolved zinc should be expressed as

$$A = \frac{Q_a}{Q_c} \times 100 (\%) \quad [3]$$

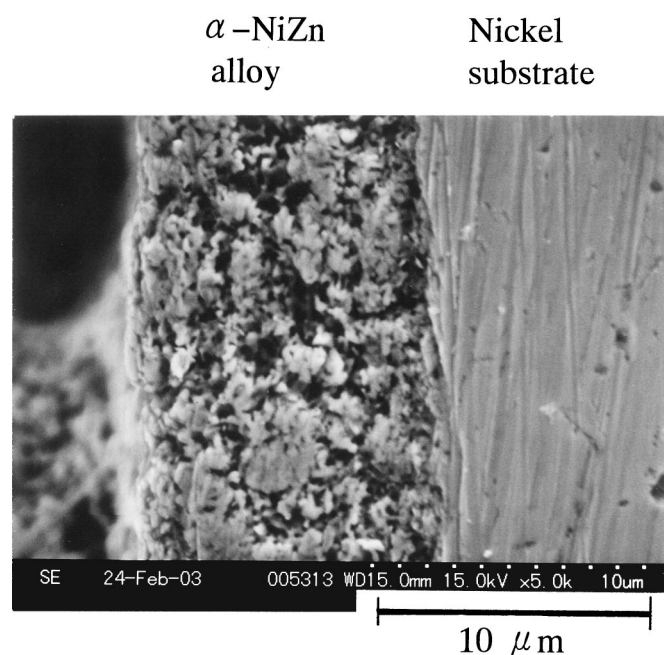


Figure 7. SEM photograph of the cross section of sample II. See the caption of Fig. 3.

Introducing $Q_c = 35 \text{ C/cm}^2$ and $Q_a = 26 \text{ C/cm}^2$ yields $A = 74\%$. In order to clarify the reason for such disagreement, experimental data are needed on the composition of alloys formed and on the current efficiencies for cathodic and anodic processes.

Although there are some uncertainties, it seems worth doing to estimate the porosity and pore size in the porous layer. Assuming that the thickness of the surface alloy layer does not change during dealloying, simple mass balance calculation yields the porosity of the α -NiZn alloy layer. Thus the nickel content in a unit volume of the original γ -NiZn alloy layer must be equal to that in the unit apparent volume of the porous α -NiZn alloy layer. Therefore,

$$W_{\text{Ni}}(\gamma)d(\gamma) = (1 - p)W_{\text{Ni}}(\alpha)d(\alpha) \quad [4]$$

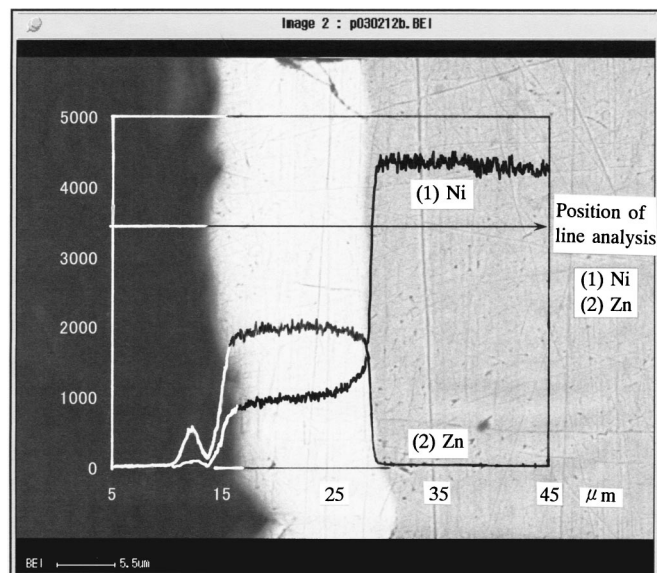


Figure 8. BEI of the cross section of sample I and Ni $K\alpha$ and Zn $K\alpha$ signals as functions of depth in EPMA.

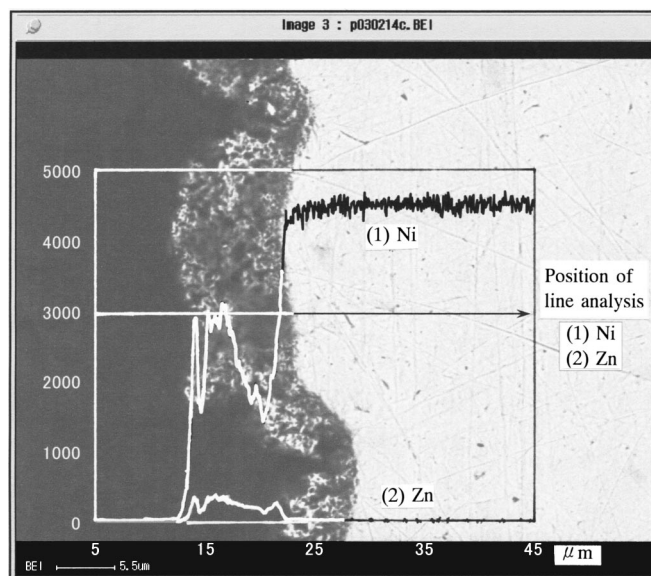


Figure 9. BEI of the cross section of sample II and Ni $K\alpha$ and Zn $K\alpha$ signals as functions of depth in EPMA.

where p is the porosity, $W_{\text{Ni}}(\gamma)$ and $W_{\text{Ni}}(\alpha)$ are the weight fractions of nickel in γ - and α -NiZn alloys, respectively, and $d(\gamma)$ and $d(\alpha)$ are the corresponding crystallographic densities. Equation 4 gives

$$p = 1 - W_{\text{Ni}}(\gamma)d(\gamma)/W_{\text{Ni}}(\alpha)d(\alpha) \quad [5]$$

Introducing the values of Table IV, the porosity is calculated to be $p = 0.82$, that is, 82%. This calculation seems fair judged by the SEM images in Fig. 6.

Assuming a simple model of cylindrical pores of diameter D and length L and perpendicular to the geometric surface of the electrode, the pore size can be estimated from the porosity and the roughness factor. If the number of pores per unit geometric area is n , then the porosity p and the roughness factor R are expressed as

$$p = \pi(D/2)^2 n \quad [6]$$

$$R = \pi D L n \quad [7]$$

Eliminating n from Eq. 6 and 7

$$D = 4Lp/R \quad [8]$$

Introducing $L = 18.5 \mu\text{m}$, $p = 0.82$, and $R = 240$, the diameter of pores is calculated to be $D = 0.25 \mu\text{m}$. Although actual pores are not cylindrical, this estimation seems reasonable in comparison with the SEM photographs of Fig. 6.

Table III. Double layer capacitance C_d and estimated roughness factor R .

| Specimen | C_d ($\mu\text{F/cm}^2$) | Roughness factor, R |
|--------------------------|---------------------------------|-----------------------|
| Ni (not electropolished) | 30 | 1 |
| Ni (electropolished) | 39 | 1.3 |
| Sample II | 7.3×10^3 | 240 |

Table IV. Compositions and densities of γ - and α -NiZn alloys.

| Alloy phase | Alloy composition | | Crystallographic density ^b d (g/cm ³) |
|----------------|--|---|--|
| | Mole fraction of nickel, ^a X_{Ni} | Weight fraction of nickel W_{Ni} | |
| γ -NiZn | 0.19 ^c | 0.174 | 7.78 |
| α -NiZn | 0.88 ^d | 0.868 | 8.66 |

^a Estimated from the Nernst equation and the Zn activity data.¹

^b Calculated from alloy compositions and lattice parameters ($a_0 = 8.931 \text{ \AA}$ for γ -NiZn and $a_0 = 3.574 \text{ \AA}$ for α -NiZn; see Table I).

^c Equilibrium composition at 0.27 V vs. RE.

^d Equilibrium composition at 0.50 V vs. RE.

Conclusions

In order to obtain a high surface area nickel electrode, cathodic and subsequent anodic treatments of nickel were conducted in a ZnCl₂-NaCl (60-40 mol %) melt at 450°C, and the following conclusions have been derived.

1. The cathodic treatment at 0.22 V vs. Zn in ZnCl₂-NaCl(sat) yields γ -NiZn alloy, which is dealloyed in the anodic treatment at 0.50 V to give α -NiZn alloy.

2. The obtained material exhibits a porous surface with roughness factor of *e.g.*, 240.

3. The thickness L , porosity p , and pore size (diameter) D of the porous layer can be estimated from the compositions of relevant alloys and the quantities of electricity in cathodic and anodic treatments. The values obtained under the conditions of the present study are: $L = 18.5 \text{ }\mu\text{m}$; $p = 0.82$; and $D = 0.25 \text{ }\mu\text{m}$.

4. The present method may be useful for producing high surface area electrodes, although further study is necessary on their performance in specified applications.

Acknowledgment

We would like to thank Professor Y. Awakura, T. Hirato, Dr. K. Murase, and T. Tanaka of Kyoto University for conducting XRF analysis, and T. Unesaki of Kyoto University for taking SEM photographs. EPMA measurements were performed by Mr. N. Tsumaki of Shimadzu Techno-Research, Inc.

Kyoto University assisted in meeting the publication costs of this article.

References

1. Y. Okano and A. Katagiri, *J. Electrochem. Soc.*, **144**, 1927 (1997).
2. R. P. Anantamula and D. B. Masson, *Metall. Trans.*, **5**, 605 (1974).
3. A. Yoshida, H. Takenishi, and A. Katagiri, Abstract 2B10, *31st Symposium on the Molten Salt Chemistry*, The Electrochemical Society of Japan (1999).
4. F. Hine, *Electrode Processes and Electrochemical Engineering*, Plenum Press, New York (1985).
5. Y. Ogata, H. Hori, M. Yasuda, and F. Hine, *J. Electrochem. Soc.*, **135**, 76 (1988).
6. D. Pletcher and F. C. Walsh, *Industrial Electrochemistry*, 2nd ed., Chapman and Hall, London (1990).
7. L. Chen and A. Lasia, *J. Electrochem. Soc.*, **138**, 3321 (1991).
8. A. Rami and A. Lasia, *J. Appl. Electrochem.*, **22**, 376 (1992).
9. J. Balej, J. Divisek, H. Schmitz, and J. Mergel, *J. Appl. Electrochem.*, **22**, 705 (1992).
10. J. Balej, J. Divisek, H. Schmitz, and J. Mergel, *J. Appl. Electrochem.*, **22**, 711 (1992).
11. S. Rausch and H. Wendt, *J. Electrochem. Soc.*, **143**, 2852 (1996).
12. Th. Borucinsky, S. Rausch, and H. Wendt, *J. Appl. Electrochem.*, **27**, 762 (1997).
13. S. Tanaka, N. Hirose, and T. Tanaki, *Denki Kagaku oyobi Kogyo Butsuri Kagaku*, **65**, 1044 (1997).
14. S. Tanaka, N. Hirose, and T. Tanaki, *J. Electrochem. Soc.*, **145**, 2477 (1999).
15. Joint Committee on Powder Diffraction Standards, Powder Diffraction Files, no. 4-0850 (Ni), and no. 6-0653 (Ni₅Zn₂₁).
16. *Gmelins Handbuch der anorganischen Chemie*, Vol. B1, System Nr. 57, Nickel, p. 32, Verlag Chemie, Weinheim (1965).
17. *Diffusion in Solid Metals and Alloys*, in Landolt-Börnstein Numerical Data and Functional Relationships in Science and Technology, New Series, Group III, Vol. 26, Fig. 102, p. 363, Fig. 103, p. 364, Springer-Verlag, Berlin (1990).
18. A. Katagiri and M. Nakata, Abstract 1465, the Electrochemical Society Meeting Abstracts, Vol. 2002-1, Philadelphia, Pennsylvania, May 12-17, 2002.